Anti-apoptotic effect of caspase inhibitors on H_2O_2-treated HeLa cells through early suppression of its oxidative stress

WOO HYUN PARK

Department of Physiology, Medical School, Research Institute for Endocrine Sciences,
Chonbuk National University, Jeonju 561-180, Republic of Korea

Abstract. Oxidative stress-induced cytotoxicity in cervical cancer cells may be of toxicological interest. In the present study, the effects of exogenous H_2O_2 on cell growth and death in HeLa cervical cancer cells were investigated, and the anti-apoptotic effects of various caspase (pan-caspase, caspase-3, -8 or -9) inhibitors on H_2O_2-treated HeLa cells were also evaluated with regard to reactive oxygen species (ROS) and glutathione (GSH) levels. Based on MTT assays, H_2O_2 inhibited the growth of HeLa cells with an IC_{50} value of ~75 μM at 24 h. H_2O_2 increased the number of dead cells and Annexin V-FITC-positive cells in the HeLa cells, which was accompanied by the activation of caspase-3 and the loss of mitochondrial membrane potential (MMP; $\Delta\Psi_m$). However, relatively higher doses of H_2O_2 induced necrosis in HeLa cells. Caspase inhibitors significantly prevented H_2O_2-induced HeLa cell death. H_2O_2 increased ROS including $O_2^{\bullet-}$ at 24 h and increased the activity of catalase in HeLa cells. H_2O_2 also increased the ROS level at 1 h, and several caspase inhibitors attenuated the increased level at 1 h but not at 6, 12 and 24 h. H_2O_2 decreased the GSH level in HeLa cells at 1 h, and several caspase inhibitors attenuated the decreased level of GSH at this time. H_2O_2 induced GSH depletion at 24 h. In conclusion, H_2O_2 inhibited the growth of HeLa cells via apoptosis and/or necrosis, which was accompanied by intracellular increases in ROS levels and GSH depletion. Caspase inhibitors are suggested to suppress H_2O_2-induced oxidative stress to rescue HeLa cells at the early time point of 1 h.

Introduction

Reactive oxygen species (ROS) are a group of oxygen moieties, which include hydrogen peroxide (H_2O_2), the superoxide anion ($O_2^{\bullet-}$) and the hydroxyl radical ($^{\bullet}OH$). Conventional theory has regarded ROS as deleterious or harmful to cells (1). However, it has become clear that ROS delicately regulate many cellular functions such as gene expression, differentiation and cell proliferation (2). They can also act as second messengers, influencing discrete signal transduction pathways in a variety of systems (3,4). ROS are continuously generated by the respiratory chain during oxidative phosphorylation in the form of the $O_2^{\bullet-}$ and/or are specifically produced by oxidases such as nicotine adenine diphosphate oxidase and xanthine oxidase (5). $O_2^{\bullet-}$ is metabolized to H_2O_2 by superoxide dismutases (SODs) (6). Moreover, H_2O_2 by catalase or glutathione (GSH) peroxidase yields O_2 and H_2O (7). Since a change in the redox state of a tissue implies an alteration in ROS generation or metabolism, cellular ROS are tightly regulated to prevent tissue damage. Oxidative stress may be the consequence of either overproduction of ROS and/or downregulation of antioxidants; this stress is believed to be responsible for a variety of pathological conditions such as inflammation, cardiovascular disease and cancer (8-11).

Compared with other members of ROS, H_2O_2 plays a pivotal role since it is able to freely travel through biological membranes to a distance of several cell diameters and interacts with ferrous iron (Fenton chemistry) causing the formation of the very aggressive and short-lived $^{\bullet}OH$. Tissue concentrations of H_2O_2 for the period of inflammation have been likely to reach close to millimolar levels whereas tiny amounts of H_2O_2 generated by NADPH oxidase are assumed to take action only in microenvironments of the plasma membrane such as lipid rafts (12,13). Nevertheless, in both cases, H_2O_2 may amend essential cellular functions of cell growth, proliferation and differentiation via altering signaling cascades and gene expression, or its higher level may lead to outcomes such as apoptosis or necrosis. Exogenous H_2O_2 is often applied as the

representative ROS in modeling oxidative stress in the cell and tissue.

The mechanism of apoptosis generally involves two signaling pathways, the mitochondrial pathway and the cell death receptor pathway (14-16). The key constituent in the mitochondrial pathway is the efflux of cytochrome c from mitochondria to the cytosol, where it subsequently forms a complex (apoptosome) with Apaf-1 and caspase-9, activating other caspases including caspase-3 and -7 (17). The cell death receptor pathway is characterized by binding cell death ligands such as TNFα and Fas and their cell death receptors, and subsequently activates caspase-8 and -3 (18,19). Particularly, cytosolic BID is cleaved by caspase-8 to generate a truncated product (tBID), which translocates to the mitochondria and decreases mitochondrial membrane potential (MMP; $\Delta\Psi_m$) resulting in release of cytochrome c. Therefore, crosstalk between both apoptotic pathways is manifested by the tBID. Caspase-3 is an executioner caspase, whose activation can systematically dismantle cells by cleaving key proteins such as poly(ADP-ribose) polymerase (PARP).

Cervical cancer is a major cause of cancer-related death in women worldwide, and the occurrence of this cancer is ascribed to changes in cancer-related genes as well as environmental events including viral infections. The carcinogenesis of cervical cancer has been known to be tightly linked to tissue inflammation mediated by ROS. Moreover, ROS influence genetic and epigenetic changes thereby modulating cellular proliferation and differentiation (11). H$_2$O$_2$-induced cytotoxicity in cervical cancer cells may be of toxicological research interest. Thus, in the present study, the effects of exogenous H$_2$O$_2$ on cell growth and death in human cervix adenocarcinoma HeLa cells were investigated and the anti-apoptotic effects of various caspase (pan-caspase, caspase-3, -8 or -9) inhibitors on H$_2$O$_2$-treated HeLa cells were evaluated in relation to changes in ROS and GSH levels.

Materials and methods

Cell culture. Human cervical adenocarcinoma HeLa cells were obtained from the American Type Culture Collection (ATCC; Manassas, VA, USA) and maintained in a humidified incubator containing 5% CO$_2$ at 37˚C. HeLa cells were cultured in RPMI-1640 supplemented with 10% fetal bovine serum (FBS) (both from Sigma-Aldrich Chemical Co., St. Louis, MO, USA) and 1% penicillin-streptomycin (Gibco-BRL, Grand Island, NY, USA). Cells were routinely grown in 100-mm plastic tissue culture dishes (Nunc, Roskilde, Denmark) and harvested with a solution of trypsin-EDTA while in a logarithmic phase of growth.

Reagents. H$_2$O$_2$ was purchased from Sigma-Aldrich Chemical Co. The pan-caspase inhibitor (Z-VAD-FMK; benzyloxycarbonyl-Val-Ala-Asp-fluoromethylketone), caspase-3 inhibitor (Z-DEVD-FMK; benzyloxycarbonyl-Asp-Glu-Val-Asp-fluoromethylketone), caspase-8 inhibitor (Z-IETD-FMK; benzyloxycarbonyl-Ile-Glu-Thr-Asp-fluoromethylketone) and caspase-9 inhibitor (Z-LEHD-FMK; benzyloxycarbonyl-Leu-Glu-His-Asp-fluoromethylketone) were obtained from R&D Systems, Inc. (Minneapolis, MN, USA) and were dissolved in dimethyl sulfoxide (DMSO; Sigma-Aldrich Chemical Co.).

Based on a previous study (20), cells were pretreated with each caspase inhibitor for 1 h prior to treatment with H$_2$O$_2$. DMSO (0.2%) was used as a control vehicle and it did not appear to affect cell growth or death.

Cell growth and cell number assays. Cell growth changes were determined by measuring the absorbance of 3-(4,5-dimethylthiazol-2-yl)-2,5-diphenyltetrazolium bromide dye (MTT; Sigma-Aldrich Chemical Co.) in living cells as described previously (21). Changes in the numbers of viable and dead cells were determined by trypan blue cell counting. In brief, 5x10^3 cells/well were seeded in 96-well microtiter plates for the MTT assays and 3x10^5 cells/well were seeded in 24-well plates (both from Nunc) for cell counting. After exposure to the indicated amounts of H$_2$O$_2$ for 24 h, the cells in the 96-well plates were used for MTT assays, and the cells in the 24-well plates were collected with trypsin digestion for trypan blue cell counting. Twenty microliters of MTT solution [2 mg/ml in phosphate-buffered saline (PBS)] was added to each well of the 96-well plates. The plates were incubated for an additional 4 h at 37˚C. Media in plates were withdrawn by pipetting, and 200 µl DMSO was added to each well to solubilize the formazan crystals. The optical density was measured at 570 nm using a microplate reader (Synergy™ 2; BioTek Instruments Inc., Winooski, VT, USA).

Analysis of cell cycle distribution and sub-G1 phase cells. Cell cycle distribution and sub-G1 cell analysis were determined by propidium iodide (PI) (Sigma-Aldrich; Ex/Em = 488/617 nm) staining. In brief, 1x10^6 cells in a 60-mm culture dish (Nunc) were incubated with the indicated amounts of H$_2$O$_2$ with or without 15 µM caspase inhibitors for 1, 6, 12 or 24 h. Total cells including floating cells were then washed with PBS and fixed in 70% (v/v) ethanol. Cells were washed again with PBS, and then incubated with PI (10 µg/ml) with simultaneous RNase treatment at 37˚C for 30 min. Cellular DNA content was measured using a FACStar flow cytometer and analyzed using Lysis II and CellFit software (both from Becton-Dickinson, Franklin Lakes, NJ, USA).

Lactate dehydrogenase (LDH) activity for the detection of necrosis. Necrosis in cells treated with H$_2$O$_2$ was evaluated using the LDH kit (Sigma-Aldrich Chemical Co.). In brief, 1x10^6 cells in a 60-mm culture dish (Nunc) were incubated with the indicated doses of H$_2$O$_2$ for 24 h. After treatment, the culture media were collected and centrifuged for 5 min at 1,500 rpm. Fifty microliters of the media supernatant was added to a fresh 96-well plate along with the LDH assay reagent and then incubated at room temperature for 30 min. The absorbance values were measured at 490 nm using a microplate reader (Synergy™ 2). LDH release was expressed as the percentage of extracellular LDH activity compared with the control cells.

Annexin V-FITC/PI staining for cell death detection. Apoptotic cell death was determined by staining the cells with Annexin V-fluorescein isothiocyanate (FITC; Invitrogen Life Technologies, Camarillo, CA, USA; Ex/Em = 488/519 nm) as previously described (22). In brief, 1x10^6 cells in a 60-mm culture dish (Nunc) were incubated with the designated

doses of H_2O_2 with or without 15 μM caspase inhibitors for 1, 6, 12 or 24 h. Cells were washed twice with cold PBS and then resuspended in 500 μl of binding buffer [10 mM HEPES/NaOH (pH 7.4), 140 mM NaCl, 2.5 mM $CaCl_2$] at a concentration of $1x10^6$ cells/ml. Annexin V-FITC (5 μl) and PI (1 μg/ml) were then added, and the cells were analyzed with a FACStar flow cytometer. Viable cells were negative for both PI and Annexin V; apoptotic cells were positive for Annexin V and negative for PI whereas late apoptotic dead cells display both high Annexin V and PI labeling. Nonviable cells, which underwent necrosis, were positive for PI and negative for Annexin V.

Measurement of mitochondrial membrane potential (MMP; $\Delta\Psi_m$). MMP ($\Delta\Psi_m$) levels were measured by Rhodamine 123 fluorescent dye (Sigma-Aldrich Chemical Co.; Ex/Em = 485/535 nm). In brief, $1x10^6$ cells in a 60-mm culture dish (Nunc) were incubated with the indicated amounts of H_2O_2 with or without 15 μM caspase inhibitors for 24 h. Cells were washed twice with PBS and incubated with Rhodamine 123 (0.1 μg/ml) at 37°C for 30 min. Rhodamine 123 staining intensity was determined by a FACStar flow cytometer (Becton-Dickinson). Rhodamine 123-negative cells indicated the loss of MMP ($\Delta\Psi_m$) in the cells.

Western blot analysis. The change in caspase-3 and PARP in H_2O_2-treated cells was determined by western blotting. In brief, $1x10^6$ cells in a 60-mm culture dish (Nunc) were incubated with the indicated amounts of H_2O_2 for 24 h. The cells were then washed in PBS and suspended in five volumes of lysis buffer [20 mM HEPES. (pH 7.9), 20% (v/v) glycerol, 200 mM KCl, 0.5 mM EDTA, 0.5% (v/v) NP-40, 0.5 mM DTT and 1% (v/v) protease inhibitor cocktail]. The protein concentrations in the supernatant were determined using the Bradford method. Samples containing 10 μg total protein were resolved by 8 or 12.5% SDS-PAGE gels, transferred to Immobilon-P PVDF membranes (Millipore, Billerica, MA, USA) by electroblotting and then probed with anti-caspase-3, anti-PARP, anti-β-actin (Santa Cruz Biotechnology, Santa Cruz, CA, USA) and anti-LC3A/B (Cell Signaling Technology, Waltham, MA, USA) antibodies. Membranes were incubated with horseradish peroxidase-conjugated secondary antibodies. Blots were developed using an ECL kit (Amersham, Arlington Heights, IL, USA).

Quantification of caspase-3 and -8 activities. The activities of caspase-3 and -8 were assessed using the Caspase-3 and Caspase-8 Colorimetric Assay Kits (R&D Systems, Inc.) as previously used (23). In brief, $1x10^6$ cells in a 60-mm culture dish (Nunc) were incubated with 100 μM H_2O_2 for 24 h. The cells were then washed in PBS and suspended in 5 volumes of lysis buffer provided in the kits. Protein concentrations were determined using the Bradford method. Supernatant samples containing 50 μg total protein were used for determination of caspase-3 and -8 activities. These were added to each well in 96-well microtiter plates (Nunc) with DEVD-pNA or IETD-pNA as caspase-3 and -8 substrates respectively at 37°C for 1 h. The optical density of each well was measured at 405 nm using a microplate reader (SpectraMax 340; Molecular Devices Co. Sunnyvale, CA,

USA). Caspase-3 and -8 activities were expressed in arbitrary absorbance units.

Detection of intracellular ROS levels. Intracellular ROS levels were detected by the fluorescent probe dye, 2',7'-dichlorodihydrofluorescein diacetate (H_2DCFDA) (Ex/Em = 495/529 nm; Invitrogen Molecular Probes, Eugene, OR, USA) at 1, 6, 12 or 24 h. H_2DCFDA is poorly selective for the superoxide anion radical ($O_2^{\bullet-}$). In contrast, dihydroethidium (DHE) (Invitrogen Molecular Probes; Ex/Em = 518/605 nm) is a fluorogenic probe that is highly selective for $O_2^{\bullet-}$ among ROS. In brief, $1x10^6$ cells/ml in FACS tube (Becton-Dickinson) were treated with 100 μM H_2O_2 with or without 15 μM caspase inhibitors in the presence of 20 μM H_2DCFDA or DHE. The fluorescence levels of DCF and DHE were evaluated using a FACStar flow cytometer at 1 h. DCF (ROS) and DHE ($O_2^{\bullet-}$) levels were expressed as mean fluorescence intensity (MFI), which was calculated by CellQuest software (Becton-Dickinson). In addition, $1x10^6$ cells in a 60-mm culture dish (Nunc) were incubated with the indicated amounts of H_2O_2 with or without 15 μM caspase inhibitors for 6, 12 and 24 h. Cells were incubated with 20 μM H_2DCFDA or DHE at 37°C for 30 min. H_2DCFDA or DHE fluorescence was assessed using a FACStar flow cytometer.

Measurement of cellular SOD and catalase activities. SOD enzyme activity was measured using the SOD assay kit-WST (Fluka Co., Milwaukee, WI, USA), and catalase enzyme activity was measured using a catalase assay kit from Sigma-Aldrich Chemical Co. In brief, $1x10^6$ cells were incubated with 100 μM H_2O_2 for 24 h. The cells were then washed in PBS and suspended in 5 volumes of lysis buffer [20 mM HEPES (pH 7.9), 20% glycerol, 200 mM KCl, 0.5 mM EDTA, 0.5% NP-40, 0.5 mM DTT and 1% protease inhibitor cocktail (from Sigma)]. The protein concentration of the supernatant was determined by the Bradford method. Supernatant samples containing 100 μg total protein were used for determination of SOD and catalase enzyme activities. These were added to each well in 96-well microtiter plates (Nunc) with the appropriate working solutions (according to the manufacturer's instructions) at 25°C for 30 min. The color changes were measured at 450 or 520 nm using a microplate reader (SpectraMax 340). The value for the experimental group was expressed as a percentage of the control group.

Detection of the intracellular GSH. Cellular GSH levels were analyzed using a 5-chloromethylfluorescein diacetate dye (CMFDA) (Invitrogen Molecular Probes; Ex/Em = 522/595 nm) at 1, 6, 12, or 24 h. In brief, $1x10^6$ cells/ml in a FACS tube (Becton-Dickinson) were treated with 100 μM H_2O_2 with or without 15 μM caspase inhibitors in the presence of 5 μM CMFDA. The level of CMF fluorescence was evaluated using a FACStar flow cytometer at 1 h. CMF (GSH) levels were expressed as MFI, which were calculated by CellQuest software. In addition, $1x10^6$ cells in a 60-mm culture dish (Nunc) were incubated with the indicated amounts of H_2O_2 with or without 15 μM caspase inhibitors for 6, 12 and 24 h. Cells were incubated with 5 μM CMFDA at 37°C for 30 min. CMF fluorescence was assessed using a FACStar flow
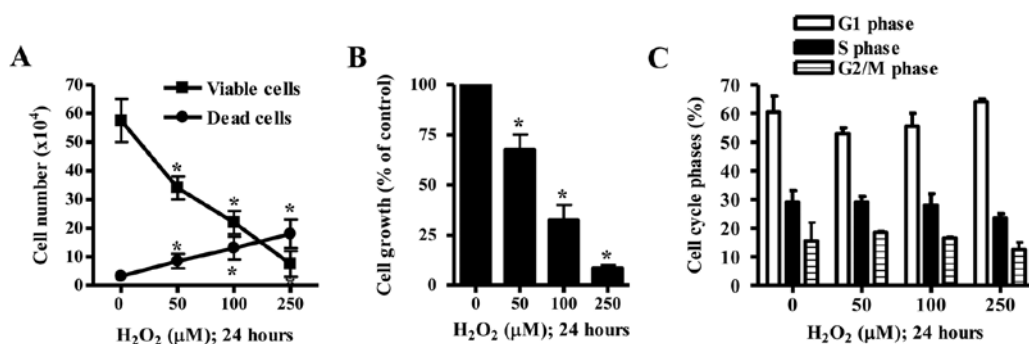
Figure 1. Effects of H_2O_2 on the cell growth in HeLa cells. Exponentially growing cells were treated with the indicated concentrations of H_2O_2 for 24 h. (A) The graph shows the numbers of viable (trypan blue-negative) and dead (trypan blue-positive) cells in the HeLa cells. (B) The graph shows the cellular growth changes in HeLa cells as assessed by MTT assays. (C) The graph shows the cell cycle distribution in HeLa cells as measured by a FACStar flow cytometer. *p<0.05 compared with the control group.
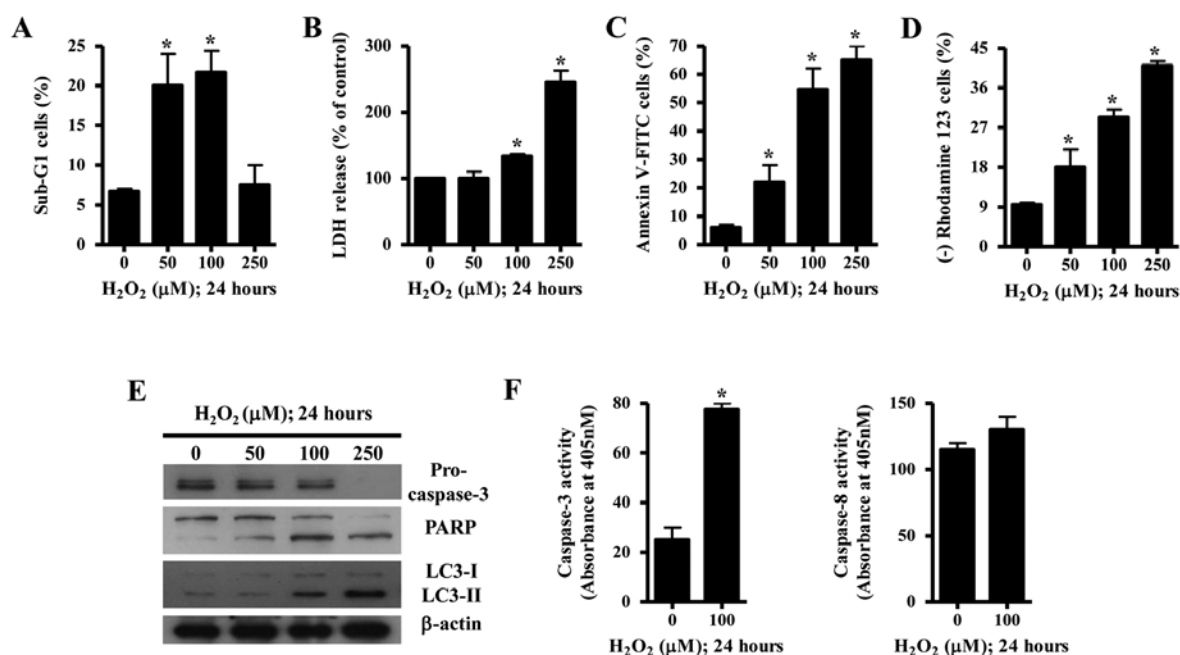

Figure 2. Effects of H_2O_2 on cell death and MMP ($\Delta\Psi_m$) in HeLa cells. Exponentially growing cells were treated with the indicated concentrations of H_2O_2 for 24 h. (A) The graph shows the percentages of sub-G1 cells in the HeLa cells as measured by FACStar flow cytometer. (B) The graph shows the percentage of LDH release when compared with that in the control cells. (C) The graph shows the percentages of Annexin V-FITC-positive cells as measured by FACStar flow cytometer. (D) The graph shows the percentages of Rhodamine 123-negative [MMP ($\Delta\Psi_m$) loss] cells as measured by FACStar flow cytometer. (E) Western blot data of the levels of pro-caspase-3, PARP and LC3 in H_2O_2-treated HeLa cells. (F) The graphs show the activities of caspase-3 and -8 in the H_2O_2-treated HeLa cells. *p<0.05 compared with the control group. MMP, mitochondrial membrane potential; LDH, lactate dehydrogenase.

cytometer. Negative CMF staining (GSH depleted) of cells was expressed as the percentage of (-) CMF cells.

Statistical analysis. The results represent the means of at least two independent experiments (means ± SD). The data were analyzed using InStat software (GraphPad Prism4; GraphPad Software, San Diego, CA, USA). The Student's t-test or one-way analysis of variance (ANOVA) with post hoc analysis using Tukey's multiple comparison test was used for parametric data. The statistical significance was defined as p<0.05.

Results

Effects of H_2O_2 on cell growth in HeLa cells. The effect of H_2O_2 on the growth of HeLa cells was examined at 24 h. Treatment with 50-250 μM H_2O_2 significantly decreased the viable (trypan blue-negative) cell number in the HeLa cells in a dose-dependent manner whereas H_2O_2 dose-dependently increased the number of dead (trypan blue-positive) cells (Fig. 1A). Based on the MTT assays, 50-250 μM H_2O_2 significantly inhibited the growth of HeLa cells with an IC_{50} (the half maximal inhibitory concentration) of ~75 μM (Fig. 1B). When the cell cycle distribution in the H_2O_2-treated HeLa cells was examined, none of the tested doses of H_2O_2 significantly induced any specific cell cycle phase arrest when compared with these parameters in the control cells (Fig. 1C).

Effects of H_2O_2 on cell death and MMP ($\Delta\Psi_m$) in HeLa cells. Next, we aimed to ascertain whether the H_2O_2-induced cell death was through apoptosis or necrosis in HeLa cells. While
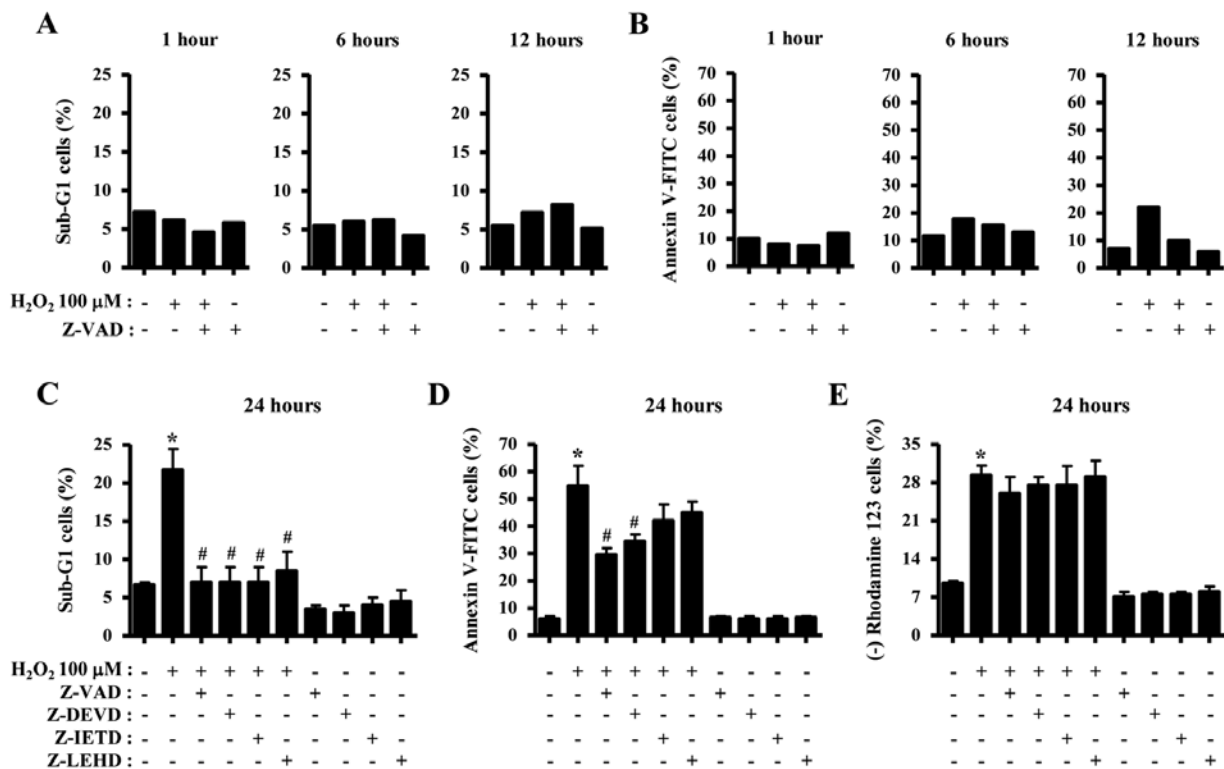
Figure 3. Effects of caspase inhibitors on apoptosis in H_2O_2-treated HeLa cells. Exponentially growing cells were treated with 100 μM H_2O_2 for the indicated times following 1 h of pre-incubation with 15 μM of a caspase inhibitor. (A and C) The graphs show the percentages of sub-G1 cells. (B and D) The graphs show the percentages of Annexin V-FITC-positive cells. (E) The graph shows the percentages of Rhodamine 123-negative [MMP ($\Delta\Psi_m$) loss] cells. $^*p<0.05$ compared with the control group. $^\#p<0.05$ compared with cells treated with H_2O_2 only. Z-VAD; pan-caspase inhibitor, Z-DEVD; caspase 3 inhibitor, Z-IETD; caspase 8 inhibitor, Z-LEHD; caspase 9 inhibitor. MMP, mitochondrial membrane potential.

50 or 100 μM H_2O_2 significantly increased the percentages of sub-G1 cells in HeLa cells, 250 μM H_2O_2 did not increase the percentages of sub-G1 cells in these cells (Fig. 2A). Since H_2O_2 can induce necrosis in HeLa cells, the status of necrosis was assessed using the LDH release assay. Treatment with 100 or 250 μM H_2O_2 significantly induced LDH release in HeLa cells at 24 h (Fig. 2B). Treatment with 50-250 μM H_2O_2 increased the numbers of Annexin V-FITC-positive cells in the HeLa cells in a dose-dependent manner (Fig. 2C). Treatment with 100 μM H_2O_2 increased the portion of apoptotic cells (Annexin V-FITC-positive/PI-negative) whereas 250 μM H_2O_2 relatively increased the portion of late apoptotic cells (Annexin V-FITC-positive/PI-positive) (data not shown). When the effect of H_2O_2 on MMP ($\Delta\Psi_m$) in HeLa cells was assessed using Rhodamine 123, H_2O_2 dose-dependently induced the loss of MMP ($\Delta\Psi_m$) (Fig. 2D). Examination of apoptosis-related protein changes during H_2O_2-induced cell death revealed that the level of pro-caspase-3 was decreased by H_2O_2 (Fig. 2E). The intact 116-kDa form of PARP was decreased by H_2O_2 whereas the cleaved form was increased (Fig. 2E). Furthermore, autophagy marker light chain 3 (LC3) was converted to LC3-II in the 100 and 250 μM H_2O_2-treated HeLa cells, indicating that H_2O_2 induced autophagy in the HeLa cells (Fig. 2E). The activity of caspase-3 was increased in H_2O_2-treated HeLa cells whereas that of caspase-8 was slightly increased (Fig. 2F).

Effects of caspase inhibitors on the apoptosis of H_2O_2-treated HeLa cells. We investigated whether caspases are required

for H_2O_2-induced apoptosis. Based on a previous study (20), HeLa cells were pretreated with 15 μM of caspase inhibitor for 1 h prior to treatment with H_2O_2. Treatment with 100 μM H_2O_2 did not significantly increase the percentages of sub-G1 cells in the HeLa cells at 1, 6 or 12 h, and the pan-caspase inhibitor (Z-VAD) did not affect the percentages at these times (Fig. 3A). H_2O_2 increased the numbers of Annexin V-FITC-positive cells in the HeLa cells at 6 and 12 h, and Z-VAD markedly reduced the number at 12 h (Fig. 3B). Moreover, treatment with all of the tested caspase inhibitors (Z-VAD, Z-DEVD for caspase-3, Z-IETD for caspase-8 and Z-LEHD for caspase-9) showed the marked rescue of HeLa cells from H_2O_2-induced cell death at 24 h, as measured by the population of sub-G1 cells (Fig. 3C). In addition, these inhibitors decreased the numbers of Annexin V-FITC-positive cells in the H_2O_2-treated HeLa cells at 24 h, and Z-VAD particularly showed a strong effect (Fig. 3D). However, none of the caspase inhibitors significantly prevented the loss of MMP ($\Delta\Psi_m$) by H_2O_2 (Fig. 3E). In relation to the 250 μM H_2O_2-treated HeLa cells, 250 μM H_2O_2 seemed to slightly increase the numbers of sub-G1 cells at 6, 12 and 24 h but not at 1 h (data not shown). Z-VAD did not decrease the numbers at these times but instead it increased the number at 12 h (data not shown). In addition, H_2O_2 increased the numbers of Annexin V-FITC-positive cells in the HeLa cells at 6, 12 and 24 h (data not shown). Z-VAD did not reduce the percentages of Annexin V-FITC-positive cells in the 250 μM H_2O_2-treated HeLa cells but it increased the number of Annexin V-FITC-positive cells in these cells at
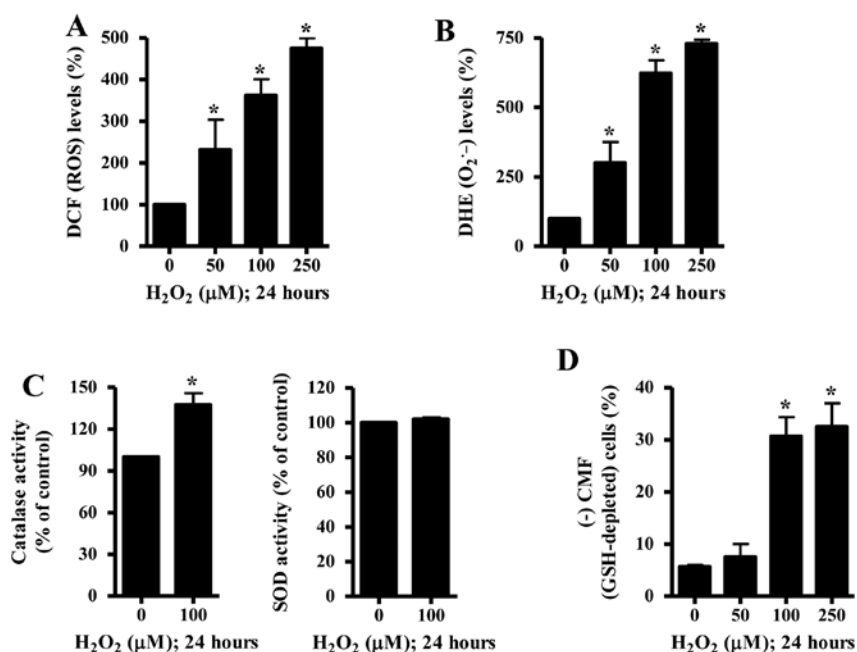
Figure 4. Effects of H_2O_2 on ROS and GSH levels in HeLa cells. Exponentially growing cells were treated with the indicated concentrations of H_2O_2 for 24 h. ROS and GSH levels in the HeLa cells were measured using a FACStar flow cytometer. (A) The graph indicates DCF (ROS) levels (%). (B) The graph indicates DHE ($O_2^{\bullet-}$) levels (%). (C) The activities of catalase and SOD were measured as described in Materials and methods. The graphs show changes in catalase and SOD activities following exposure to 100 μM H_2O_2. (D) The graph indicates the (-) CMF (GSH-depleted) cells (%) in the HeLa cells when compared with the control cell group. *p<0.05 compared with the control group. ROS, reactive oxygen species; GSH, glutathione.

24 h (data not shown). These results indicated that the caspase inhibitors did not protect HeLa cell death induced by 250 μM H_2O_2.

Effects of H_2O_2 on intracellular ROS and GSH levels in HeLa cells. To assess the intracellular ROS levels in the H_2O_2-treated HeLa cells, H_2DCFDA and DHE dyes were used. All the tested doses of H_2O_2 increased the ROS (DCF) level in the HeLa cells at 24 h (Fig. 4A). The level of DHE fluorescence dye, which specifically reflects $O_2^{\bullet-}$ accumulation in cells, was also increased in the H_2O_2-treated HeLa cells (Fig. 4B). Furthermore, the activities of SOD and catalase in the H_2O_2-treated HeLa cells were measured. As shown in Fig. 4C, 100 μM H_2O_2 increased the activity of catalase but did not alter the activity of SOD. Following the measurement of intracellular GSH levels in the H_2O_2-treated HeLa cells using a CMFDA dye, 100 or 250 μM H_2O_2 increased the GSH-depleted cell number in HeLa cells at 24 h while 50 μM H_2O_2 did not significantly induce GSH depletion (Fig. 4D).

Effects of caspase inhibitors on ROS and GSH levels in the H_2O_2-treated HeLa cells. To determine whether the levels of intracellular ROS and GSH in the H_2O_2-treated HeLa cells were altered by treatment with each caspase inhibitor, ROS and GSH levels in the HeLa cells were assessed at the early time point of 1 h and at the extended time point of 24 h (Fig. 5). The intracellular ROS (DCF) level was increased in the H_2O_2-treated cells at 1 h (Fig. 5A). Z-VAD, caspase-3 and -9 inhibitors seemed to attenuate the increased ROS (DCF) level by H_2O_2, and all the caspase inhibitors decreased the basal level of ROS (DCF) in the HeLa control cells (Fig. 5A). At 24 h, none of the caspase inhibitors significantly affected the

ROS (DCF) level in the H_2O_2-treated HeLa cells (Fig. 5D). Additionally, Z-VAD did not attenuate the increased ROS (DCF) level by H_2O_2 at 6 and 12 h (data not shown). Treatment with 100 μM H_2O_2 did not alter the DHE ($O_2^{\bullet-}$) level in the HeLa cells at 1 h (Fig. 5B). Z-VAD decreased the DHE ($O_2^{\bullet-}$) level in the H_2O_2-treated and -untreated HeLa cells at 1 h, and other caspase inhibitors reduced the basal level of DHE ($O_2^{\bullet-}$) in the HeLa control cells (Fig. 5B). In addition, Z-VAD among the caspase inhibitors decreased the DHE ($O_2^{\bullet-}$) level in H_2O_2-treated HeLa cells at 24 h (Fig. 5E). In regards to the GSH levels, 100 μM H_2O_2 decreased the GSH level in HeLa cells at 1 h (Fig. 5C). Caspase-3 and -9 inhibitors including Z-VAD attenuated the decreased GSH level by H_2O_2, and all inhibitors except the caspase-9 inhibitor reduced the basal level of GSH in the HeLa control cells at 1 h (Fig. 5C). At 24 h, Z-VAD prevented GSH depletion in the H_2O_2-treated HeLa cells (Fig. 5F).

Discussion

Exogenous H_2O_2 was applied for inducing oxidative stress in HeLa cervical cancer cells. After exposure to H_2O_2 for 24 h, the IC_{50} value in the HeLa cells was ~75 μM based on MTT assays. H_2O_2 dose-dependently increased the number of dead cells and Annexin V-FITC-positive cells in the HeLa cells, suggesting that H_2O_2-induced HeLa cell death occurred via apoptosis. Evidently, H_2O_2 decreased the level of pro-caspase-3 and induced the cleavage of PARP proteins in the HeLa cells. The activity of caspase-3 was also increased in the H_2O_2-treated HeLa cells. However, 250 μM H_2O_2 did not significantly increase the percentages of sub-G1 cells in the HeLa cells, implying that the relatively higher dose of H_2O_2
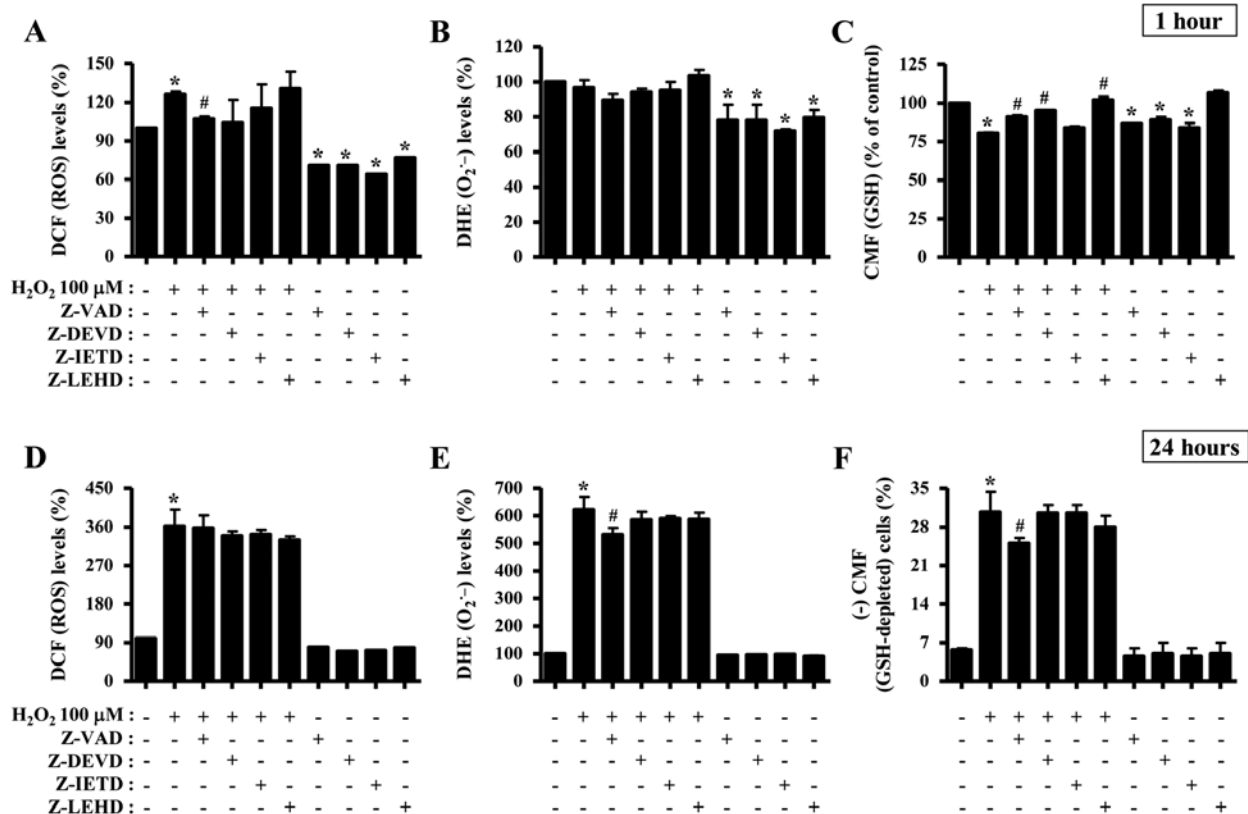
Figure 5. Effects of caspase inhibitors on ROS and GSH levels in H_2O_2-treated HeLa cells. Exponentially growing cells were treated with 100 μM H_2O_2 for 1 or 24 h following 1 h pre-incubation of 15 μM of a caspase inhibitor. ROS and GSH levels in HeLa cells were measured using a FACStar flow cytometer. (A and D) Graphs indicate DCF (ROS) levels (%) at (A) 1 h and (D) 24 h. (B and E) Graphs indicate DHE ($O_2^{•-}$) levels (%) at (B) 1 h and (E) 24 h. (C and F) The graphs indicate mean CMF (GSH) levels (%) at (C) 1 h and (-) CMF (GSH-depleted) cells (%) in HeLa cells compared with control cell group at (F) 24 h. *p<0.05 compared with the control group. #p<0.05 compared with cells treated with H_2O_2 only. ROS, reactive oxygen species; GSH, glutathione.

fixed HeLa cells similar to ethanol or methanol. In addition, 100 or 250 μM H_2O_2 significantly induced LDH release in the HeLa cells at 24 h. Therefore, H_2O_2 appeared to provoke HeLa cell death via apoptosis as well as necrosis depending on its concentration. Moreover, autophagy appeared to be involved in H_2O_2-induced HeLa cell death since LC3-I was converted to LC3-II in these cells. Apoptosis is closely related to the collapse of MMP ($\Delta\Psi_m$) (24). This result demonstrated that H_2O_2 triggered the loss of MMP ($\Delta\Psi_m$) in HeLa cells in a dose-dependent manner, suggesting that HeLa cell death by H_2O_2 was tightly correlated with the collapse of MMP ($\Delta\Psi_m$). Moreover, it has been reported that ROS may have roles in cell cycle arrest and progression via regulating cell cycle-related proteins (25,26). However, H_2O_2 did not induce any specific phase arrest of the cell cycle in HeLa cells, suggesting that H_2O_2-induced oxidative stress did not have an effect on particular proteins related to cell cycle arrest and progression.

Treatment with the caspase inhibitors tested in this experiment significantly prevented HeLa cell death by H_2O_2, and Z-VAD showed a stronger effect on reducing apoptosis. In particular, although H_2O_2 slightly increased the activity of caspase-8, its inhibitor significantly prevented HeLa cell death by H_2O_2. Thus, a subtle change in the activity of caspase-8 seemed to strongly affect the pro-apoptotic pathway in H_2O_2-treated HeLa cells. These data suggest that

the mitochondrial pathway and cell death receptor pathway are together necessary for the complete induction of apoptosis in H_2O_2-treated HeLa cells. However, Wu et al suggested that H_2O_2-induced apoptosis in HeLa cells is not through mitochondria-dependent caspase-9 activation (27). The exact apoptotic pathway(s) and the caspase(s) directly involved in the H_2O_2-induced apoptosis in HeLa cells warrant further studied. With regard to the MMP ($\Delta\Psi_m$), caspase inhibitors did not prevent the loss of MMP ($\Delta\Psi_m$) induced by H_2O_2. In addition, caspase inhibitors also did not recover the decreased MMP ($\Delta\Psi_m$) level in the H_2O_2-treated HeLa cells (data not shown). These results imply that the loss of MMP ($\Delta\Psi_m$) following treatment with H_2O_2 activated caspases and consequently induced apoptosis. In addition, the activation of caspase by H_2O_2 did not positively intensify the MMP ($\Delta\Psi_m$) loss. Furthermore, the loss of MMP ($\Delta\Psi_m$) by H_2O_2 may not be enough to fully trigger apoptosis in HeLa cells under the inhibition of caspase activity.

The ROS level was significantly increased in HeLa cells treated with H_2O_2 at 24 h. Since H_2O_2 did not decrease the activity of SOD and increased the activity of catalase at 24 h, increases in ROS levels including $O_2^{•-}$ were likely to occur via their strong generation rather than the lack of scavenging them. In addition, it is possible that exogenous H_2O_2 strongly generates $O_2^{•-}$ via the damage of mitochondria, and both H_2O_2 and $O_2^{•-}$ can be efficiently converted into the toxic $^{•}OH$ via

the Fenton reaction to kill HeLa cells. However, H_2O_2 did not increase the $O_2^{\cdot-}$ (DHE) level in HeLa cells at 1 h, suggesting that it did not affect the mitochondrial respiratory transport chain and the activity of various oxidases to generate $O_2^{\cdot-}$ within this early time point. Moreover, caspase inhibitors showing the prevention of H_2O_2-induced cell death failed to significantly decrease the ROS level including $O_2^{\cdot-}$ at 6, 12 and 24 h. However, Z-VAD, caspase-3 and -8 inhibitors appeared to attenuate the increased ROS (DCF) level by H_2O_2 at 1 h. In addition, all of the caspase inhibitors decreased the basal level of ROS including $O_2^{\cdot-}$ in the HeLa control cells. It is conceivable that the reduced basal activity of caspase by their inhibitors improves the reliability of antioxidant-related enzymes to strongly scavenge basal intracellular ROS in HeLa cells. Therefore, the early suppression of H_2O_2-induced oxidative stress by caspase inhibitors seems to be crucial for the protection of HeLa cells against it. The exact role of each caspase inhibitor in preventing H_2O_2-induced HeLa cell death still needs to be defined further.

GSH is a main non-protein antioxidant in cells. Apoptotic effects are inversely comparable to the GSH content (28-30). Likewise, H_2O_2 was found to increase the number of GSH-depleted cells in HeLa cells at 24 h. In addition, Z-VAD partially prevented GSH depletion in H_2O_2-treated HeLa cells. These results support the notion that the intracellular GSH content has a decisive effect on cell death (29,31,32). However, 50 μM H_2O_2, the dose at which apoptosis is induced in HeLa cells, did not significantly allow GSH depletion in these cells. Moreover, the other caspase inhibitors except Z-VAD failed to prevent GSH depletion in the H_2O_2-treated HeLa cells. Therefore, the loss of GSH content seemed to be necessary but not sufficient for the induction of apoptosis in the H_2O_2-treated HeLa cells. Treatment with 100 μM H_2O_2 decreased the GSH level at 1 h. The decreased GSH level was likely to be due to its use for the decrease in ROS (DCF) level at this time. In addition, caspase-3 and -9 inhibitors partially recovered the GSH level in the H_2O_2-treated HeLa cells, implying that these caspase inhibitors seemed to positively maintain the GSH content in these cells. Without the incubation of H_2O_2, caspase inhibitors except for the caspase-9 inhibitor reduced the basal level of GSH in the HeLa control cells at 1 h. Thus, these results suggest that each caspase inhibitor differentially regulated the intracellular GSH levels in HeLa cells depending on the presence or absence of H_2O_2.

In conclusion, H_2O_2 inhibited the growth of HeLa cells via apoptosis and/or necrosis, which was accompanied by intracellular ROS increase and GSH depletion. The anti-apoptotic effect of caspase inhibitors on H_2O_2-induced HeLa cell death may result from the early suppression of H_2O_2-induced oxidative stress. The present data provide useful information for the understanding of the toxicological effect of exogenous H_2O_2 on HeLa cells.

Acknowledgements

References

1. Gonzalez C, Sanz-Alfayate G, Agapito MT, Gomez-Niño A, Rocher A and Obeso A: Significance of ROS in oxygen sensing in cell systems with sensitivity to physiological hypoxia. Respir Physiol Neurobiol 132: 17-41, 2002.
2. Baran CP, Zeigler MM, Tridandapani S and Marsh CB: The role of ROS and RNS in regulating life and death of blood monocytes. Curr Pharm Des 10: 855-866, 2004.
3. Irani K: Oxidant signaling in vascular cell growth, death, and survival: a review of the roles of reactive oxygen species in smooth muscle and endothelial cell mitogenic and apoptotic signaling. Circ Res 87: 179-183, 2000.
4. Perez-Vizcaino F, Cogolludo A and Moreno L: Reactive oxygen species signaling in pulmonary vascular smooth muscle. Respir Physiol Neurobiol 174: 212-220, 2010.
5. Zorov DB, Juhaszova M and Sollott SJ: Mitochondrial ROS-induced ROS release: an update and review. Biochim Biophys Acta 1757: 509-517, 2006.
6. Zelko IN, Mariani TJ and Folz RJ: Superoxide dismutase multigene family: a comparison of the CuZn-SOD (SOD1), Mn-SOD (SOD2), and EC-SOD (SOD3) gene structures, evolution, and expression. Free Radic Biol Med 33: 337-349, 2002.
7. Wilcox CS: Reactive oxygen species: roles in blood pressure and kidney function. Curr Hypertens Rep 4: 160-166, 2002.
8. Chen TJ, Jeng JY, Lin CW, Wu CY and Chen YC: Quercetin inhibition of ROS-dependent and -independent apoptosis in rat glioma C6 cells. Toxicology 223: 113-126, 2006.
9. Dasmahapatra G, Rahmani M, Dent P and Grant S: The tyrphostin adaphostin interacts synergistically with proteasome inhibitors to induce apoptosis in human leukemia cells through a reactive oxygen species (ROS)-dependent mechanism. Blood 107: 232-240, 2006.
10. Wallach-Dayan SB, Izbicki G, Cohen PY, Gerstl-Golan R, Fine A and Breuer R: Bleomycin initiates apoptosis of lung epithelial cells by ROS but not by Fas/FasL pathway. Am J Physiol Lung Cell Mol Physiol 290: L790-L796, 2006.
11. Sarsour EH, Kumar MG, Chaudhuri L, Kalen AL and Goswami PC: Redox control of the cell cycle in health and disease. Antioxid Redox Signal 11: 2985-3011, 2009.
12. Rhee SG, Kang SW, Jeong W, Chang TS, Yang KS and Woo HA: Intracellular messenger function of hydrogen peroxide and its regulation by peroxiredoxins. Curr Opin Cell Biol 17: 183-189, 2005.
13. Vilhardt F and van Deurs B: The phagocyte NADPH oxidase depends on cholesterol-enriched membrane microdomains for assembly. EMBO J 23: 739-748, 2004.
14. Shi Y: Mechanisms of caspase activation and inhibition during apoptosis. Mol Cell 9: 459-470, 2002.
15. Ashkenazi A and Dixit VM: Death receptors: signaling and modulation. Science 281: 1305-1308, 1998.
16. Budihardjo I, Oliver H, Lutter M, Luo X and Wang X: Biochemical pathways of caspase activation during apoptosis. Annu Rev Cell Dev Biol 15: 269-290, 1999.
17. Mehmet H: Caspases find a new place to hide. Nature 403: 29-30, 2000.
18. Hengartner MO: The biochemistry of apoptosis. Nature 407: 770-776, 2000.
19. Liu X, Yue P, Zhou Z, Khuri FR and Sun SY: Death receptor regulation and celecoxib-induced apoptosis in human lung cancer cells. J Natl Cancer Inst 96: 1769-1780, 2004.
20. Han YH, Kim SZ, Kim SH and Park WH: Pyrogallol inhibits the growth of lung cancer Calu-6 cells via caspase-dependent apoptosis. Chem Biol Interact 177: 107-114, 2009.
21. Han YH and Park WH: Tiron, a ROS scavenger, protects human lung cancer Calu-6 cells against antimycin A-induced cell death. Oncol Rep 21: 253-261, 2009.
22. Han YH, Moon HJ, You BR and Park WH: The effect of MG132, a proteasome inhibitor on HeLa cells in relation to cell growth, reactive oxygen species and GSH. Oncol Rep 22: 215-221, 2009.
23. Park WH, Han YH, Kim SH and Kim SZ: Pyrogallol, ROS generator inhibits As4.1 juxtaglomerular cells via cell cycle arrest of G2 phase and apoptosis. Toxicology 235: 130-139, 2007.
24. Yang J, Liu X, Bhalla K, et al: Prevention of apoptosis by Bcl-2: release of cytochrome c from mitochondria blocked. Science 275: 1129-1132, 1997.

25. Han YH, Kim SH, Kim SZ and Park WH: Antimycin A as a mitochondria damage agent induces an S phase arrest of the cell cycle in HeLa cells. Life Sci 83: 346-355, 2008.
26. Han YH, Kim SZ, Kim SH and Park WH: Pyrogallol inhibits the growth of human lung cancer Calu-6 cells via arresting the cell cycle arrest. Toxicol In Vitro 22: 1605-1609, 2008.
27. Wu Y, Wang D, Wang X, *et al*: Caspase 3 is activated through caspase 8 instead of caspase 9 during H_2O_2-induced apoptosis in HeLa cells. Cell Physiol Biochem 27: 539-546, 2011.
28. Han YH, Kim SZ, Kim SH and Park WH: Enhancement of arsenic trioxide-induced apoptosis in HeLa cells by diethyl-dithiocarbamate or buthionine sulfoximine. Int J Oncol 33: 205-213, 2008.
29. Estrela JM, Ortega A and Obrador E: Glutathione in cancer biology and therapy. Crit Rev Clin Lab Sci 43: 143-181, 2006.
30. Han YH, Kim SZ, Kim SH and Park WH: Suppression of arsenic trioxide-induced apoptosis in HeLa cells by N-acetylcysteine. Mol Cells 26: 18-25, 2008.
31. Han YH, Kim SH, Kim SZ and Park WH: Carbonyl cyanide *p*-(trifluoromethoxy) phenylhydrazone (FCCP) as an $O_2(^{\bullet-})$ generator induces apoptosis via the depletion of intracellular GSH contents in Calu-6 cells. Lung Cancer 63: 201-209, 2009.
32. Han YH, Kim SZ, Kim SH and Park WH: Intracellular GSH level is a factor in As4.1 juxtaglomerular cell death by arsenic trioxide. J Cell Biochem 104: 995-1009, 2008.